"Cerium Incorporated Copper Oxide and It's Surface Modification with Biopolymers: Synthesis, Insight Characterizations and Surface Activity Studies Towards the Extraction of Chromium(VI) and Arsenic(III) from Their Contaminated Aqueous Phases"

Summary of Work (5000 Words)

For the Award of Ph. D. (Sc.) Degree in Chemistry

Submitted to

Presidency University

PRESIDENCY UNIVERSITY
KOLKATA

By

Ayan Ghosh

Registration No.: R-18RS205110192

Date of Registration: 09/01/2021

Department Of Chemistry

Presidency University

2024

Supervisor

Dr. Palani Sasikumar

Assistant Professor

Department of Chemistry, Presidency University

Kolkata 700073, India

4/3/25

Allowed to submit the thesis for Ph.D. degree

4/3/25

04/03/25

04/03/25

04.03.25

04/03/25

4/3/25

Table of Content

Title	Page No.
1. Introduction	**4-11**
1.1. Water Pollution: An environmental threat	
1.2. Remediation Processes	
1.3. Nanomaterials as adsorbents for water treatment	
1.4. Research background	
1.5. Aim and objectives of the present work	
2. Materials and Methods	**12-15**
2.1. Chemical Reagents and Apparatus	
2.2. Synthesis of adsorbents	
2.2.1. Preparation of hydrous Ce(IV) incorporated Cu(II) oxide (HCCO)	
2.2.2. Preparation of chitosan cross-linked hydrous Ce(IV) incorporated Cu(II) oxide (CHCCO)	
2.3. Experimental procedures	
3. Results and Discussion	**15-19**
3.1. Adsorbent characterization of HCCO	
3.2. Adsorbent characterization of CHCCO	
4. Batch Adsorption Study	**19-27**
4.1. Equilibrium analysis	
4.1.1. Adsorption isotherm model study for Cr(VI) adsorption by HCCO	
4.1.2. Adsorption isotherm study for As(III) adsorption by HCCO	
4.1.3. Adsorption isotherm study for Cr(VI) adsorption by CHCCO	

5. Summary	**27-28**
6. Acknowlwdgement	**28**
7. References	**28-32**
8. List of Publictions	**32-33**
9. National and International Seminar, Conference & Workshop Presentation	**33-34**

1. Introduction

1.1. Water Pollution: An environmental threat

Water pollution is a multifaceted environmental challenge that encompasses a wide array of contaminants, including toxic metal ions, which pose significant threats to both ecosystems and human health. Among these pollutants, toxic metal ions such as chromium, arsenic, mercury, cadmium, and lead feature prominently due to their persistence, bioaccumulative nature, and detrimental effects on living organisms. Industrial activities, mining operations, agricultural practices, and improper waste disposal are primary sources of metal ion pollution in water bodies worldwide. For instance, industrial processes like metal smelting, electroplating, and mining release substantial amounts of metal ions into the environment through effluents and runoff. Similarly, agricultural activities involving the use of metal-based pesticides and fertilizers contribute to metal contamination of water sources through surface runoff and leaching into groundwater. Additionally, natural processes such as weathering of rocks and volcanic activity can release metals into water bodies, albeit in lower concentrations compared to anthropogenic sources. The presence of toxic metal ions in water can have severe consequences for aquatic ecosystems. These pollutants can accumulate in sediments, bioaccumulate in aquatic organisms, and biomagnify along the food chain, leading to ecosystem disruption and biodiversity loss. Human exposure to metal ion pollution in water sources poses significant risks to public health. Drinking water contaminated with metals such as chromium, arsenic, lead, and cadmium can have serious health consequences, including neurological disorders, developmental delays in children, organ damage, and increased cancer risk. Moreover, vulnerable populations living in proximity to industrial facilities or in areas with poor water quality infrastructure are disproportionately affected by metal ion pollution, exacerbating existing environmental justice concerns.

1.2. Remediation Processes

Various methods have been developed to eliminate harmful toxicants such as arsenic, chromium, and fluoride etc. from water. These methods include ion exchange, precipitation coagulation, membrane separation processes, electrolysis, electrodialysis, and adsorption. Each method presents its own set of advantages and disadvantages, which are outlined in Table 1. Among these techniques, adsorption stands out as the most widely utilized and

effective method for removing these pollutants from water, owing to its high affinity and capacity, cost-effectiveness, operational efficiency across a wide pH range, simplicity of design, and versatility.

Table 1. Different remediation processes with advantages and disadvantages

Methods	Advantages	Disadvantages	References
Membrane Separation Process	• Membranes provide an effective barrier to suspended solids, all inorganic pollutants, organic micro-pollutants, pesticides etc. • It ensures constant water quality. • It works under wide pH range. • No interference by other ions is observed. • The process simple, automated and minimal manpower is required.	• It removes all the ions present in water, though some minerals are essential for proper growth, remineralization is required after treatment. • The process is expensive in comparison to other options.	[1]
Electrolysis	• Simple equipment. • Convenient operation. • Non-requirement of chemical substances for the sedimentation. • Electrochemically oxidize or reduce the organic contaminants to non-hazardous inorganic substances.	• High energy consumption. • Less efficient. • High operational cost.	[2]
Coagulation –	• Produced sludge with good	• Increased sludge	[3]

precipitation	sludge settling and dewatering characteristics. • The process if simple.	volume generation. • Cannot treat wastewater wholly and must be followed by other treatment techniques for better results.	
Ion- Exchange Method	• Removal efficiency is very high. • Retains the taste and colour of water intact.	• The cost is high as synthetic resin is used. • The technique is expensive because of the cost of resin, pretreatment required to maintain the pH, regeneration and waste disposal. • Regeneration of resin is a problem • Treated water has a very low pH and high levels of chloride.	[4]
Adsorption	• The process can remove contaminants with an efficiency as high as 90%. • Treatment is cost-effective. • Operation is simple.	• The process is highly dependent on pH. • The regeneration is required after some time. • Low selectivity.	[5]

1.3. Nanomaterials as adsorbents for water treatment

Nanomaterials are materials with dimensions on the nanometer scale, typically ranging from 1 to 100 nm. At this scale, materials exhibit unique physical, chemical, and biological properties that are distinct from their bulk counterparts. These properties arise due to quantum confinement, increased surface area-to-volume ratio, and surface effects, making nanomaterials highly desirable for a wide range of applications across various fields. Nanomaterials can be categorized into different types based on their composition, structure, and properties. Some common types include nanocomposites (materials composed of two or more nanoscale components), nanoparticles (nanosized particles), nanotubes (cylindrical nanostructures with nanoscale diameters), nanowires (ultrafine wires with nanoscale diameters), and quantum dots (nanoscale semiconductor particles with quantum mechanical properties).

These materials find applications in diverse areas such as environmental remediation, electronics, medicine, energy, catalysis, and nanotechnology. Due to their unique properties and wide-ranging applications, nanomaterials are the subject of extensive research and development efforts worldwide, with ongoing exploration into novel synthesis methods, characterization techniques, and applications to address various technological challenges and societal needs. Nano-adsorbents, with their high surface area and reactivity, offer promising solutions for the removal of toxic contaminants like arsenic, chromium, and other toxic ions from water. Arsenic, a notorious carcinogen, is often present in groundwater, while chromium is a common industrial pollutant. Nano-adsorbents, typically nanoparticles or nanocomposites, enhance adsorption capacity and efficiency due to their increased surface-to-volume ratio and unique surface properties.

For arsenic removal, nano-adsorbents like iron oxide nanoparticles, titanium dioxide nanotubes, or nanostructured adsorbents based on metal oxides have shown efficacy. These materials offer active sites for arsenic binding through surface complexation or ion exchange mechanisms. In the case of chromium, nano-adsorbents such as zero-valent iron nanoparticles, graphene oxide, or metal-organic frameworks have demonstrated excellent adsorption capabilities. The high reactivity and specific surface chemistry of these materials facilitate the reduction of toxic chromium (VI) to less harmful chromium (III) species, enhancing removal efficiency.

Overall, nano-adsorbents offer a promising avenue for the removal of arsenic and chromium contaminants from water, providing a cost-effective and environmentally friendly solution to water purification challenges. However, further research is necessary to optimize their synthesis, performance, and scalability for widespread application in water treatment processes.

1.4. Research background

Over the years, sorption techniques have emerged as a widely applied method for the removal of toxic contaminants such as chromium (Cr(VI)) and arsenic (As(III)) from aqueous environments. These techniques utilize the chemical (chemisorption), physical (physisorption), and biological (bioremediation) properties of sorbents, capitalizing on the suspended nature of these contaminants in water. A broad spectrum of sorbent materials has been investigated for their effectiveness in removing such hazardous ions. These materials include nanocomposites, polymeric composites, nanoparticles, and bio-sorbents, all of which have shown varying degrees of success in addressing the issue of water contamination. Among these, a range of widely recognized adsorbents has been proposed specifically for the removal of Cr(VI) and As(III) from water. These adsorbents include metal oxide and mixed metal oxide-based materials, polymer and biopolymer composites, biochar-based substances, graphene-based materials, granular activated carbon, zeolites, and layered double hydroxides. Each of these materials offers unique characteristics that make them suitable for adsorbing toxic ions, with their specific properties tailored to the adsorption process. In particular, the application of nanosized metals and metal oxides has garnered substantial attention due to their cost-effectiveness and impressive performance. Transition metals such as iron, copper, and manganese, as well as rare metals like cerium and zirconium, have been the focus of increasing research efforts. These metals are particularly valued for their strong affinity and high selectivity towards chromium and arsenic ions, making them highly effective for water treatment. Metal oxide-based composites stand out as especially promising due to their exceptional adsorption potential for these contaminants. One of the key advantages of metal oxide-based materials lies in the presence of numerous hydroxyl groups on their surfaces. These hydroxyl groups facilitate interactions with toxic ion species, enabling the ions to be adsorbed onto the material's surface. In addition to their high adsorption efficiency, these materials are non-toxic and exhibit low solubility in water, which further enhances their suitability for water treatment applications. Consequently, metal oxide nanocomposites have emerged as an excellent option for the removal of toxic metal ions from real wastewater

systems on a global scale. Their unique combination of affordability, environmental safety, and superior performance underscores their potential as a vital solution for addressing the persistent issue of water contamination.

Table 2. Comparison of adsorption capacity for chromate removal on various adsorbents at different pH

Adsorbents	pH	q_e ($mg.g^{-1}$)	References
Hydrous zirconium incorporated cerium oxide (HZICO)	3	97.04	[6]
Manganese oxide incorporated ferric oxide nanocomposite (MIFN)	3	47.8	[7]
Hydrous zirconium oxide(HZO)	2	61-66	[8]
Crystalline hydrous ferric oxide (CHFO)	2	35.7	[9]
Mesoporous iron-zirconium oxide (MIZO)	5	59.9	[10]
Fe/Cu nanoparticles (Fe/Cu NPs)	3	20.5	[11]
CuO nanoparticles	3	86.25	[12]
Mg/Al LDH	1	12.7±0.2	[13]
CeO_2 nanoparticles	7	121.9	[14]
Fe/Mn mixed oxides nanocomposites	2	26.3	[15]
Zirconium-chitosan composite (Zr-CTS)	5	175	[16]
Functionalized chitosan-Al_2O_3@SiO_2 composite (FCAS)	3	671.14	[17]
Titanium–chitosan composite (Ti–CTS)	5	171	[18]
Chitosan@SiO_2@TiO_2 nanocomposite	3	182.43	[19]
Magnetic $MnFe_2O_4$/chitosan nanocomposites (MCNC)	5	35.2	[20]

Table 3. Comparison of adsorption capacity for As(III) adsorption on various adsorbents at different pH

Adsorbents	pH	q_e ($mg.g^{-1}$)	References
Porous CeO_2–ZrO_2 nanospheres	6.9±0.2	9.2	[21]
Titanium(IV) oxide (TiO_2)	7	104	[22]
Cupric oxide nanoparticles	8±0.1	26.9	[23]
Hydrous cerium oxide nanoparticles (HCO)	7	170	[24]
Ce–Ti hybrid oxide	6.5	6.8	[25]
Iron–zirconium (Fe–Zr) binary oxide	7	120	[26]
Fe/Cu Nanoparticles	7	19.68	[27]
Fe–Ni binary oxide	7±0.1	168.6	[28]
Titanium(IV)-manganese(IV) binary oxide	7	107	[29]
S-doped copper- lanthanum bimetallic oxide (S-CuLaO)	6	314.91	[30]
Nanostructured zirconium–manganese binary hydrous oxide	5	104	[31]
Crystalline Hydrous Ferric Oxide (CHFO)	6	33.33	[32]
Bimetal iron(III)–titanium(IV) oxide (NHITO)	7±0.1	85	[33]
Nanostructured Fe-Ti-Mn composite oxide (FTMO)	7±0.1	122.3	[34]
Iron–chitosan composites	7	16.15±0.32	[35]

1.5. Aim and objectives of the present work

The current research aims to develop cost-effective, non-toxic, and innovative mixed metal oxide-based inorganic materials that can serve as highly effective adsorbents for removing chromate and arsenite ions from contaminated water. The study is structured around several primary objectives to achieve this overarching goal:

i. The focus is on the development, synthesis, and characterization of a binary hydrous [Ce(IV)-Cu(II)] oxide, referred to as HCCO. This phase involves a detailed examination of various physicochemical properties, including the material's purity, crystallinity, surface morphology, particle size, and surface area. Additionally, we analyze its thermal stability and surface charge densities across different pH levels, while also determining its isoelectric point. These attributes are critical for understanding the adsorbent's overall efficiency and its interactions with contaminants in water.

ii. The surface modification of HCCO using chitosan is undertaken with the specific aim of broadening its utility, particularly for the removal of hexavalent chromium (Cr(VI)) ions. This modification is expected to enhance the adsorbent's selectivity and adsorption capacity while contributing to its sustainability through improved regeneration potential. Chitosan was chosen as a modifier due to its eco-friendly nature, biocompatibility, and established affinity for heavy metal ions.

iii. The research includes an in-depth investigation of the adsorption behavior of the prepared adsorbent. This aspect explores how various parameters—such as the initial concentration of contaminants, temperature, adsorbent dose, pH, contact time, and stirring speed—affect adsorption. Detailed studies of adsorption kinetics and isotherms are conducted to understand the underlying mechanisms, accompanied by thermodynamic studies assessing the feasibility and spontaneity of the process. Additionally, the effects of foreign ions on adsorption efficiency are studied to determine the adsorbent's selectivity in real-world scenarios. Regeneration studies are also included to evaluate the reusability and cost-effectiveness of the material.

Through these systematic and thorough investigations, the study seeks to provide a robust solution to the pressing issue of water contamination, specifically concerning chromate and arsenite ions, while ensuring the sustainability and scalability of the developed adsorbent.

2. Materials and Methods

2.1. Chemical Reagents and Apparatus

Table 4 provides a comprehensive list of the ingredients and chemicals utilized in the synthesis of adsorbents, in the preparation of various stock solutions, and in the batch adsorption experiments. All compounds used in this study were of analytical grade and applied without further purification. Double-deionized water was used throughout the experiments. Before use, all glassware was washed with a dilute HNO_3 solution, followed by thorough rinsing with double-distilled water and acetone to ensure the removal of any contaminants.

Table 4. List of the chemicals along with their formulas, molecular weight and company names

Name of Chemicals	Chemical formula	Molecular weight ($g.mol^{-1}$)	Company name
Copper(II) acetate monohydrate	$(CH_3COO)_2Cu.H_2O$	199.65	Merck
Ammonium cerium(IV) nitrate	$(NH_4)_2Ce(NO_3)_6$	548.22	Merck
Potassium dichromate	$K_2Cr_2O_7$	294.19	Qualigens
Sodium arsenite	$NaAsO_2$	129.91	LobaChemie
1,5-diphenyl carbazide	$C_{13}H_{14}N_4O$	242.28	Merck
Silver diethyldithiocarbamate	$C_5H_{10}AgNS_2$	256.14	VWR Chemicals
Tin(II) chloride dihydrate	$SnCl_2.2H_2O$	225.63	Merck
Potassium iodide	KI	166	Merck
Lead(II) acetate trihydrate	$(CH_3COO)_2.3H_2O$	379.34	Merck
Chitosan	$C_{12}H_{24}N_2O_9$	340.33	Alfa Aesar
Glutaraldehyde	$C_5H_8O_2$	100.12	Merck
Sodium chloride	NaCl	58.44	Merck
Sodium nitrate	$NaNO_3$	84.99	Merck

Sodium hydrogen carbonate	$NaHCO_3$	84.01	Merck
Sodium sulfate	Na_2SO_4	142.04	Merck
Anhydrous iron(III) chloride	$FeCl_3$	162.21	Merck
Disodium hydrogen phosphate	Na_2HPO_4	177.99	Merck
Calcium nitrate tetrahydrate	$Ca(NO_3)_2.4H_2O$	236.15	Merck
Magnesium nitrate hexahydrate	$Mg(NO_3)_2.6H_2O$	256.41	Merck
Zinc fillings	Zn	65.39	Merck
Sodium hydroxide	NaOH	39.997	Merck
Hydrochloric acid	HCl, >98.0%	36.46	Merck
Nitric acid	HNO_3 70%	63.01	Merck
Sulfuric acid	H_2SO_4	98.079	Merck
Chloroform	$CHCl_3$	119.378	Merck

2.2. Synthesis of adsorbents

2.2.1. Preparation of hydrous Ce(IV) incorporated Cu(II) oxide (HCCO)

The synthesis of hydrous cerium-copper hybrid oxide was carried out using a chemical precipitation method that involved varying the mole ratios of Ce(IV) and Cu(II). The process began by mixing aqueous solutions of ammonium cerium(IV) nitrate and copper(II) acetate in glass vessels, adjusting their volumes to achieve the desired Ce(IV)/Cu(II) mole ratio. These solutions were stirred with a magnetic stirrer for 15 minutes to ensure intimate mixing. Following this, a 1.0 M NaOH solution was gradually added dropwise to the mixture under continuous stirring until the pH of the solution reached between 7.0 and 8.0. This addition of NaOH initiated hydrolysis, resulting in a gel-like mass of mixed hydroxides that was left undisturbed in the mother liquid for 24 hours, allowing it to stabilize. After the 24-hour period, the mother liquid was removed by filtration, leaving a green solid residue on the filter paper. This residue was thoroughly washed several times with deionized water to ensure the complete removal of any remaining nitrate and acetate ions, which could interfere with subsequent applications. Once washed, the solid was dried

at room temperature to retain its structural integrity without excessive dehydration. The dried material was then carefully ground and sieved to obtain particles within a size range of 140 to 290 μm. These processed particles were stored for use in batch sorption experiments, where they would serve as an active material for studies on ion uptake and adsorption. This method allowed for precise control over the material's composition and structure, making it suitable for applications requiring high-performance sorption capabilities.

2.2.2. Preparation of chitosan cross-linked hydrous Ce(IV) incorporated Cu(II) oxide (CHCCO)

The synthesis of chitosan cross-linked ceria-incorporated hydrous copper(II) oxide bio-polymeric composite (CHCCO) involves a two-step in situ process. In the first step, varying amounts of chitosan (ranging from 0.1 g to 0.6 g) are separately dissolved in 10 mL of a 2% (v/v) aqueous acetic acid solution. These chitosan solutions are then added dropwise into reaction vessels containing a mixture of 50 mL of ammonium cerium(IV) nitrate [$(NH_4)_2Ce(NO_3)_6$] and 50 mL of copper(II) acetate [$Cu(CH_3COO)_2$] while stirring at 400 rpm for 30 minutes to ensure a homogeneous mixture. Subsequently, the pH is gradually adjusted to between 7.0 and 8.0 by adding a 1.0 M NaOH solution dropwise, promoting the formation of a stable solution.

In the second step, 5 mL of a 5% glutaraldehyde solution is added to each reaction mixture, and stirring is continued for an additional 3 hours to complete the cross-linking process. The resulting dark green precipitate is filtered from the solution using a suction device, washed thoroughly six times with double-distilled water to remove impurities, and then dried at room temperature for 3 days. Once dried, the bio-composite is screened to a particle size between 140–290 μm, making it ready for adsorption experiments. This synthesis method effectively incorporates cerium and copper into a chitosan-based matrix, with glutaraldehyde cross-linking providing structural stability to the composite.

2.3. Experimental procedures

The study examined the adsorption of chromate and toxic heavy metal ions using a batch adsorption technique designed to evaluate how various factors, such as adsorbent dosage, adsorption kinetics, and isotherms, affect adsorption capacity. The experiments aimed to determine the adsorbent’s maximum adsorption capacity by using a controlled setup: a fixed amount of adsorbent was added to 50 mL of an adsorbate solution with a precisely known

initial concentration (C_0, $mg.L^{-1}$) in a capped 250 mL polyethylene bottle. Before each experiment, the solution's pH was adjusted to the desired level using either 0.1 M HCl or 0.1 M NaOH. Each reaction mixture was then placed in a thermostat shaker set to a constant temperature and agitated at a rate of 250 (± 5) rpm for a set time. After agitation, the solid adsorbent was separated from the liquid phase by filtration with a 0.45 µm Whatman® membrane filter, and the remaining concentration of the adsorbate in the filtrate was measured to determine the adsorption capacity (q_e, $mg.g^{-1}$) and removal percentage using the following mass balance equations Eq. 1 and Eq. 2 respectively

$$q_e = \frac{(C_0 - C_e) \times V}{m} \quad (1)$$

$$\%\ Removal = \frac{(C_0 - C_e)}{C_0} \times 100 \quad (2)$$

Where C_0 and C_e are the initial adsorbate concentration and equilibrium adsorbate concentration respectively ($mg.L^{-1}$). V is the total volume of solution (L) and m denotes the weight of the adsorbent (g).

3. Results and Discussion

3.1. Adsorbent characterization of HCCO

The analysis of primary experimental data, based on the mole variation of Ce(IV) and Cu(II), demonstrated that the optimal composition of the HCCO material was achieved with a molar ratio of 1:4 (Ce: Cu). This optimized material underwent extensive characterization to evaluate its structural and chemical properties. The surface morphology of the synthesized HCCO material was examined in detail and is depicted in Figure 1(a). The microstructural analysis revealed that the surface of the material consisted of irregularly shaped particles with sharp edges and a rough texture, suggesting that the material possesses a robust and stable architecture. This morphology is indicative of the material's potential for applications requiring mechanical and structural resilience. Additionally, energy-dispersive X-ray spectroscopy (EDX) was employed to confirm the elemental composition of the material. As shown in Figure 1(b), the EDX spectrum provided clear evidence of the presence of cerium

(Ce) and copper (Cu), confirming the successful incorporation of these elements in the HCCO structure. Further chemical characterization was carried out using Fourier-transform infrared (FTIR) spectroscopy, as illustrated in Figure 1(c). The FTIR spectrum of HCCO exhibited a broad absorption band in the wave number range of 3300–3568 cm^{-1}, which was attributed to O-H bond stretching. This confirmed the presence of both free –OH groups and hydrogen-bonded –OH groups from adsorbed water molecules. Additionally, the spectrum displayed distinct peaks at 1351.18 cm^{-1} and 889.41 cm^{-1}, which corresponded to Cu-OH bond vibrations [36]. The strong peaks observed at 1048.55 cm^{-1} and 1389.46 cm^{-1} were associated with Ce-OH bending vibrations [37], further validating the incorporation of cerium and copper hydroxyl bonds in the HCCO structure. The crystallinity of the HCCO material was investigated through powder X-ray diffraction (XRD) analysis, with the diffraction pattern presented in Figure 1(d). The XRD pattern displayed numerous sharp and intense peaks within the diffraction angle range of 10–90°, confirming the highly crystalline nature of the material. This high degree of crystallinity is a desirable feature, as it enhances the material's stability and performance in various applications. In addition to structural and chemical analysis, the specific surface area (SSA) and porosity properties of HCCO were assessed using the Brunauer-Emmett-Teller (BET) method. The N_2 adsorption-desorption isotherm, shown in Figures 1(e) and 1(f), exhibited a slight hysteresis, which is characteristic of mesoporous materials. Quantitative analysis of the BET data revealed that the specific surface area of HCCO was 13.502 $m^2.g^{-1}$, while the total pore volume was measured as 0.055 $cm^3.g^{-1}$, and the average pore radius was determined to be 17.023 Å. These results demonstrated the mesoporous nature of the material, as well as its moderate surface area and porosity, which are critical properties for potential applications requiring efficient adsorption or catalytic activity. Together, these findings highlight the structural robustness, high crystallinity, and mesoporous characteristics of the HCCO material, making it a promising candidate for a wide range of applications.

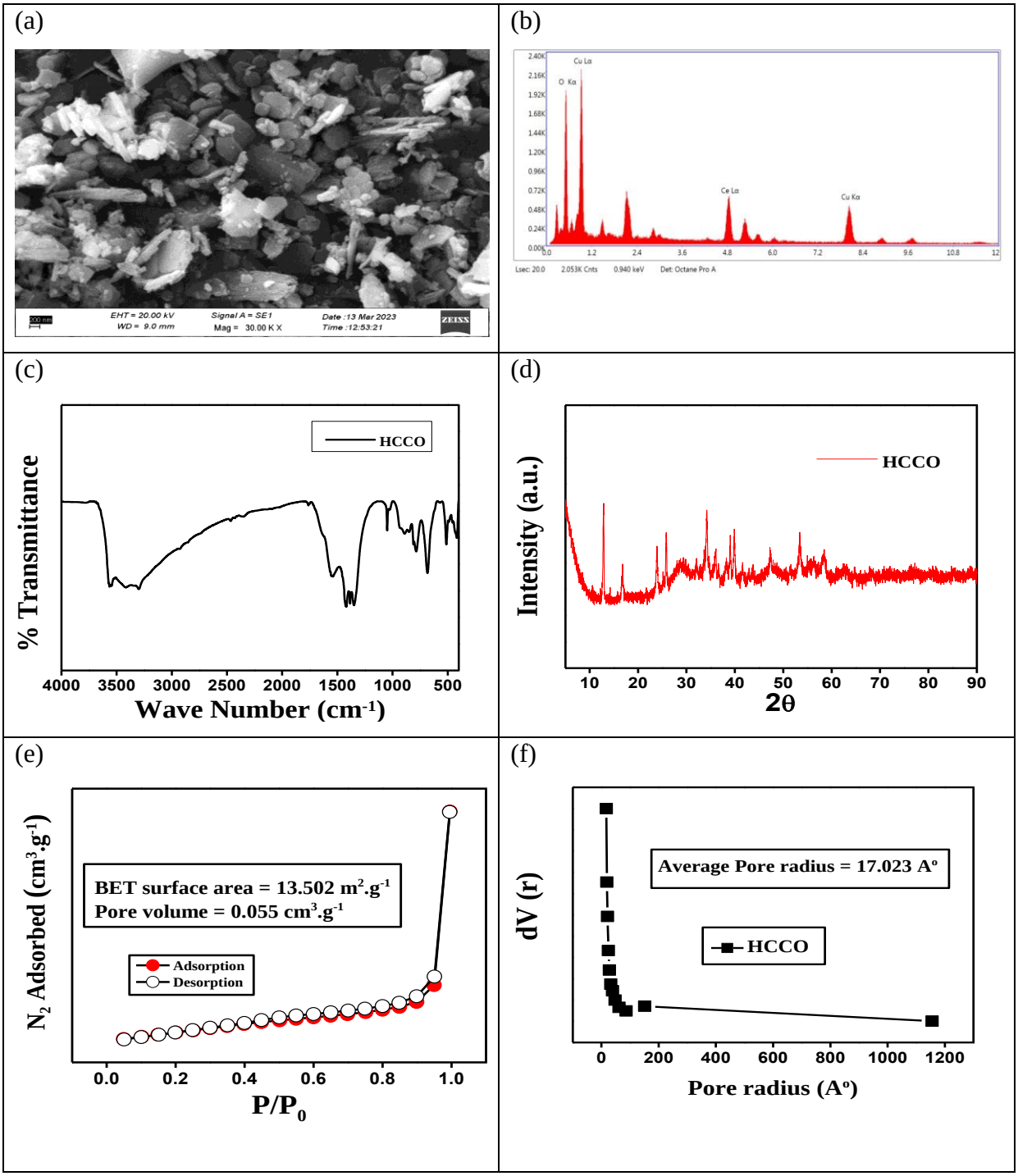

Fig. 1. (a) SEM images of HCCO at 200 nm magnification, (b) SEM-EDAX spectra of HCCO, (c) FTIR spectrum of HCCO, (d) Powder XRD pattern of HCCO, (e) BET surface area plot of HCCO, (f) Pore size distribution plot of HCCO.

3.2. Adsorbent characterization of CHCCO

The characterization of the CHCCO composite material was conducted using FTIR spectroscopy, XRD analysis, and morphological studies, providing detailed insights into its structural and compositional properties. The FTIR spectrum of the composite, shown in

Figure 2(a), revealed several distinct peaks associated with specific functional groups. The broad peak at 3414 cm^{-1} was attributed to the overlapping stretching vibrations of N-H and O-H groups, indicating the presence of these functional groups in the material. A peak observed at 2923 cm^{-1} corresponded to the C-H stretching vibrations associated with the methyl or methylene groups found in chitosan. Additionally, the peak at 1606 cm^{-1} was assigned to the bending vibrations of O-H and NH_2 groups [38]. The signal at 1384 cm^{-1} was identified as the C-H symmetric bending vibration related to the symmetrical deformation of CH_3 groups. Further, an absorption band at 1055 cm^{-1} was attributed to the skeletal C-O stretching vibrations, which are characteristic of the composite material. Peaks at lower wavenumbers, specifically at 614 cm^{-1} and 524 cm^{-1}, were linked to the vibrational bands of Ce-O and Cu-O, respectively, confirming the involvement of these bonds in the composite structure. The XRD analysis of the CHCCO composite, as depicted in Figure 2(b), revealed five distinct diffraction peaks at 2θ values of 28.68°, 35.62°, 38.75°, 48.08°, and 56.66°. These peaks were indicative of the crystalline nature of the material, particularly the presence of Ce(IV) and Cu(II) species. The sharpness and intensity of these peaks further emphasized the crystalline structure of these metal species within the composite matrix. The surface morphology of the CHCCO material was examined and is illustrated in Figure 2(c). The study revealed that the composite consisted of irregularly shaped particles with rough surface textures. This irregular morphology could potentially enhance the surface area of the material, contributing to its functional properties as an adsorbent. Furthermore, the presence of chitosan in the composite was confirmed through the EDAX spectrum analysis, shown in Figure 2(d), which displayed a peak corresponding to carbon. This provided additional evidence of chitosan's integration into the CHCCO composite matrix. Together, these analytical techniques confirmed the structural, compositional, and morphological characteristics of the CHCCO composite, highlighting its potential applications in various functional domains.

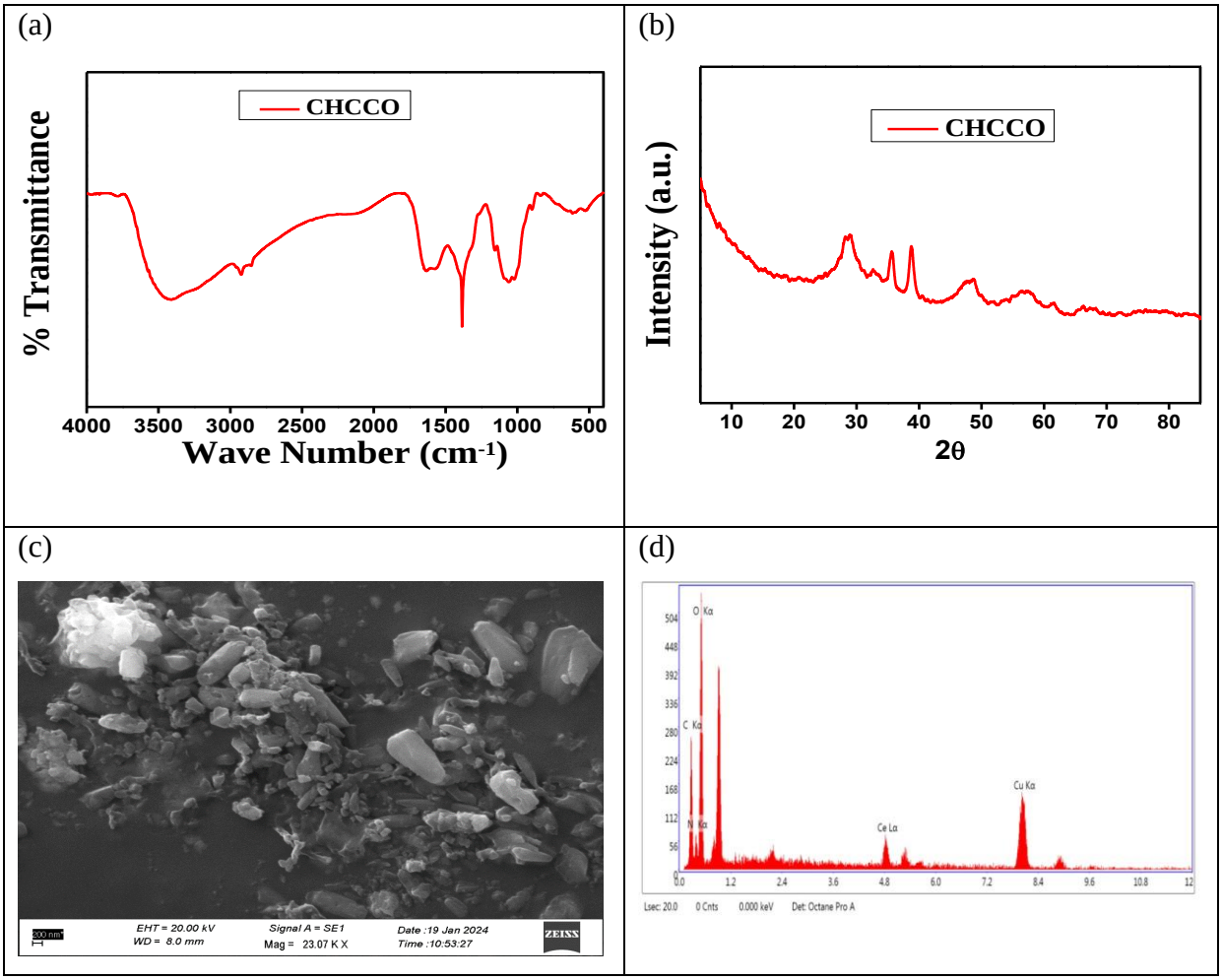

Fig. 2.(a) FTIR spectrum of CHCCO, (b) Powder XRD pattern of CHCCO, (c) SEM images of CHCCO at 200 nm magnification, (d) SEM-EDAX spectra of CHCCO.

4. Batch Adsorption Study

4.1. Equilibrium analysis

Adsorption isotherm studies are essential for understanding the mechanistic pathways of adsorption reactions on adsorbent surfaces and determining the maximum adsorption capacity of the material. These studies provide a detailed examination of the equilibrium relationship between the concentration of the adsorbate in solution and the amount adsorbed onto the adsorbent, offering critical insights into the adsorption process's efficiency and behavior under varying conditions. In this research, adsorption experiments were conducted at four different temperatures—283 K, 293 K, 303 K, and 313 K—to investigate how temperature influences the adsorption process. A wide range of adsorbate solution concentrations was

utilized to capture comprehensive adsorption behavior. The experiments were performed under controlled conditions, maintaining a consistent pH and fixed aging time to ensure the accuracy and reliability of the collected data. The equilibrium adsorption data were represented graphically by plotting the equilibrium adsorption capacity (q_e) against the equilibrium concentration of the adsorbate in solution (C_e).

To analyze the experimental equilibrium data, three widely recognized isotherm models were employed: the Langmuir, Freundlich, and Redlich-Peterson models. The Langmuir model assumes that adsorption occurs as a monolayer on a uniform surface with identical adsorption sites and no interactions between adsorbed molecules. The non-linear equation of Langmuir isotherm is

$$q_e = \frac{q_m K_L C_e}{1+K_L C_e} \quad (3)$$

Where q_e is the amount ($mg.g^{-1}$) of adsorbate adsorbed per gram of the adsorbent at equilibrium, C_e is the adsorbate concentration at equilibrium ($mg.L^{-1}$), q_m is the maximum monolayer adsorption capacity ($mg.g^{-1}$), K_L is the equilibrium constant that is connected to the energy of adsorption ($L.mg^{-1}$).

In contrast, the Freundlich model is an empirical approach that accounts for adsorption on heterogeneous surfaces with varying site energies, allowing for the possibility of multilayer adsorption.

Freundlich isotherm equation is given by

$$q_e = K_F \times C_e^{\frac{1}{n}} \quad (4)$$

K_F is the Freundlich adsorption capacity ($mg^{1-1/n}.L^{n}.g^{-1}$) and 1/n is a constant related to adsorption intensity.

The Redlich-Peterson model combines aspects of both Langmuir and Freundlich theories, making it applicable to systems that exhibit mixed characteristics of homogeneous and heterogeneous surface adsorption. The Redlich-Peterson model equation is expressed as

$$q_e = \frac{AC_e}{1+BC_e^{g}} \quad (5)$$

In this equation, the constants A and B are specific to the adsorption system being studied. These constants are experimentally determined and represent fundamental properties of the adsorbate and adsorbent, such as their interaction affinity and adsorption capacity. Additionally, the parameter g, a dimensionless variable, plays a pivotal role in shaping the model's behavior. Its value, which ranges from 0 to 1, dictates the extent to which the Redlich-Peterson model aligns with other established isotherm models, thereby providing flexibility in capturing different adsorption characteristics.

4.1.1. Adsorption isotherm model study for Cr(VI) adsorption by HCCO

The equilibrium data were analyzed using the previously mentioned isotherm models, as illustrated in Fig. 3 (a) to (c). The relevant parameters derived from the analysis using Origin software are summarized in Table 5. Upon examining the regression coefficient (R^2) values, it was observed that the Freundlich model provided a slightly better fit to the experimental isotherm data compared to the Langmuir model, although the fit to the Langmuir monolayer model was also satisfactory. This observation suggests that the active sites on HCCO were more heterogeneous than homogeneous, indicating that the reduction of Cr(VI) concentration in the aqueous medium predominantly occurred through multilayer adsorption. To further verify the enhanced fit of the Freundlich model, the equilibrium data were also assessed using the Redlich-Peterson model. The findings corroborated the earlier results, as the parameter g from the Redlich-Peterson model remained significantly below unity, supporting the predominance of heterogeneous adsorption behavior. Additionally, an increase in both the Freundlich constant (K_F) and the Langmuir monolayer saturation capacity (q_m) was observed as the temperature increased from 283 K to 313 K. This trend highlights that HCCO exhibits strong potential as a chromate-scavenging material. The high adsorption capacity of HCCO further underscores its effectiveness in removing Cr(VI) from waste acidic water. Moreover, the enhanced adsorption capacity observed with increasing temperature suggests that the adsorption process is endothermic. This thermodynamic characteristic reinforces the suitability of HCCO for efficient Cr(VI) extraction in industrial and environmental applications.

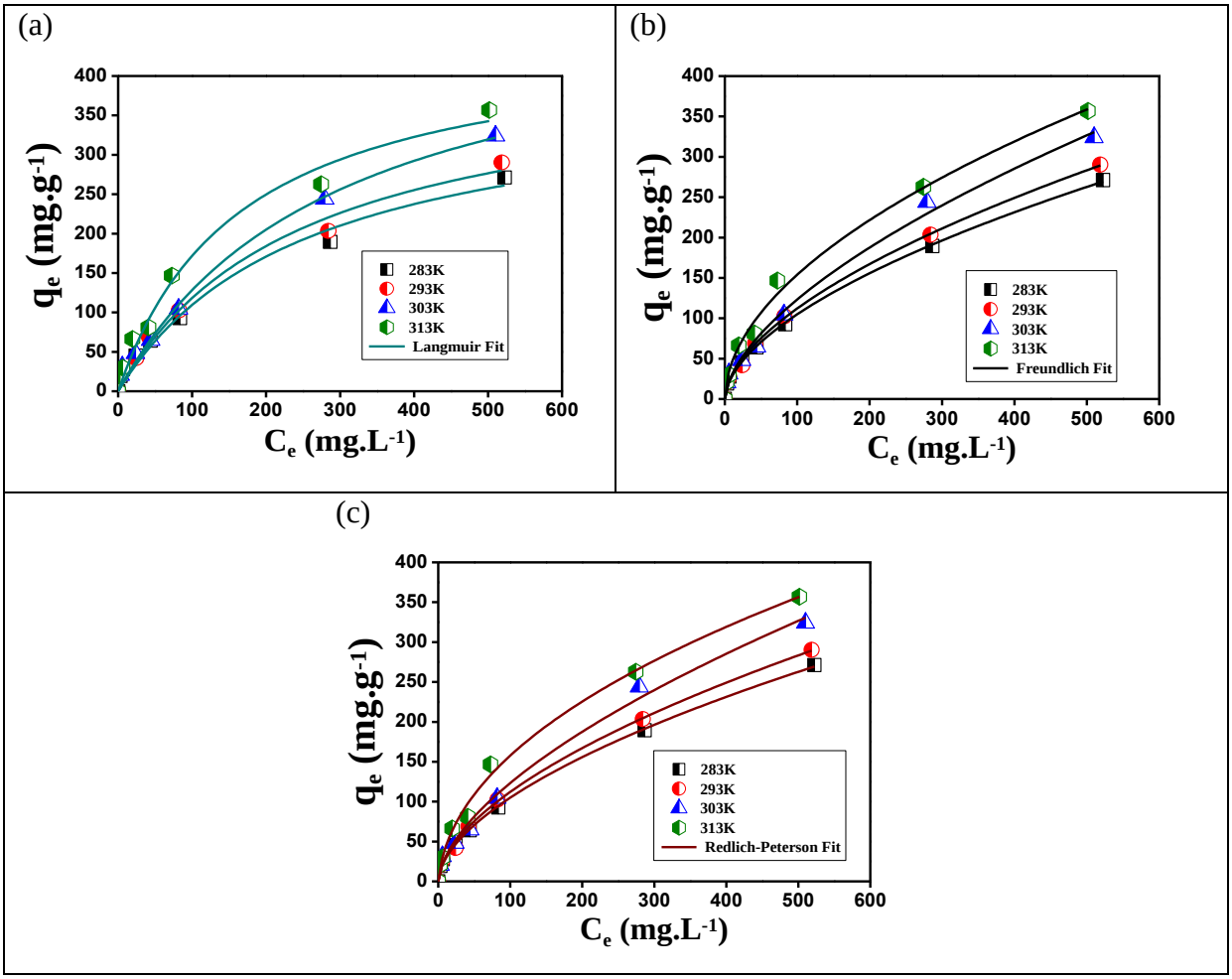

Fig. 3. Plots of the equilibrium data relating on Cr(VI) adsorption for scavenging from water by HCCO at pH 3.0 and; the non-linear model fittings of data with (a) Langmuir, (b) Freundlich, (c) Redlich-Peterson model isotherms.

Table 5. Isotherm equation parameters estimated on Cr(VI) adsorption for scavenging from water by HCCO at pH 3.0 and four different temperatures.

Isotherm	Parameters	283K	293K	303K	313K
Freundlich	**K_F(mg$^{1-1/n}$ L^n g^{-1})**	7.583	7.898	7.593	13.701
	n	1.753	1.735	1.652	1.903
	R^2	0.998	0.998	0.993	0.994
Langmuir	**q_m(mg g^{-1})**	388.648	415.609	508.853	455.813
	K_L(L mg^{-1})×10^2	0.392	0.398	0.338	0.605
	R^2	0.979	0.983	0.989	0.984

Redlich-	**A**	1.766×10^{8}	3.025×10^{8}	1.030×10^{8}	0.692
Peterson	**B**	1.339×10^{9}	2.389×10^{9}	7.823×10^{9}	14.362
	g	0.429	0.423	0.394	0.534
	R^2	0.998	0.997	0.992	0.994

4.1.2. Adsorption isotherm study for As(III) adsorption by HCCO

The isotherm data were comprehensively analyzed using nonlinear methods, employing the previously introduced equations (Eqs. 3–5) and processed using Origin software for precise modeling. The analysis involved fitting the experimental data to three different isotherm models: Langmuir, Freundlich, and Redlich–Peterson, with the results illustrated in Figures 4(a), 4(b), and 4(c), respectively. This approach enabled a detailed comparison of the adsorption behavior of As(III) on the adsorbent surface under varying conditions. The parameters obtained from these nonlinear analyses are tabulated in Table 5, providing a quantitative basis for evaluating the performance of each model. An examination of the linear regression coefficients (R^2) in Table 5 reveals that the equilibrium data exhibit a stronger correlation with the Langmuir model compared to the Freundlich model. This outcome suggests that the adsorption of As(III) predominantly follows a monolayer adsorption mechanism on the adsorbent surface, as predicted by the Langmuir isotherm. The high degree of fit underscores the relevance of this model in accurately describing the adsorption behavior. Furthermore, the Langmuir model predicts a maximum adsorption capacity of 164.011 $mg.g^{-1}$ at 283 K, reflecting the excellent capability of the adsorbent to effectively remove As(III) under the specified conditions.

In addition to the Langmuir and Freundlich models, the Redlich–Peterson model was also evaluated, and its findings further corroborate the monolayer adsorption mechanism. The g factor derived from the Redlich–Peterson model remained consistently close to 1 across all four temperatures investigated. This consistency reinforces the conclusion that the adsorption of As(III) on the adsorbent occurs through a monolayer process, characterized by uniform adsorption sites and minimal surface heterogeneity.

Overall, the results of this study highlight the strong adsorption performance of the adsorbent material for the removal of As(III). The adherence of the experimental data to the Langmuir model, supported by the insights from the Redlich–Peterson model, provides a clear understanding of the adsorption mechanism. The high adsorption capacity, combined with the

precision of the modeling, underscores the potential of this adsorbent for effective As(III) remediation in practical applications.

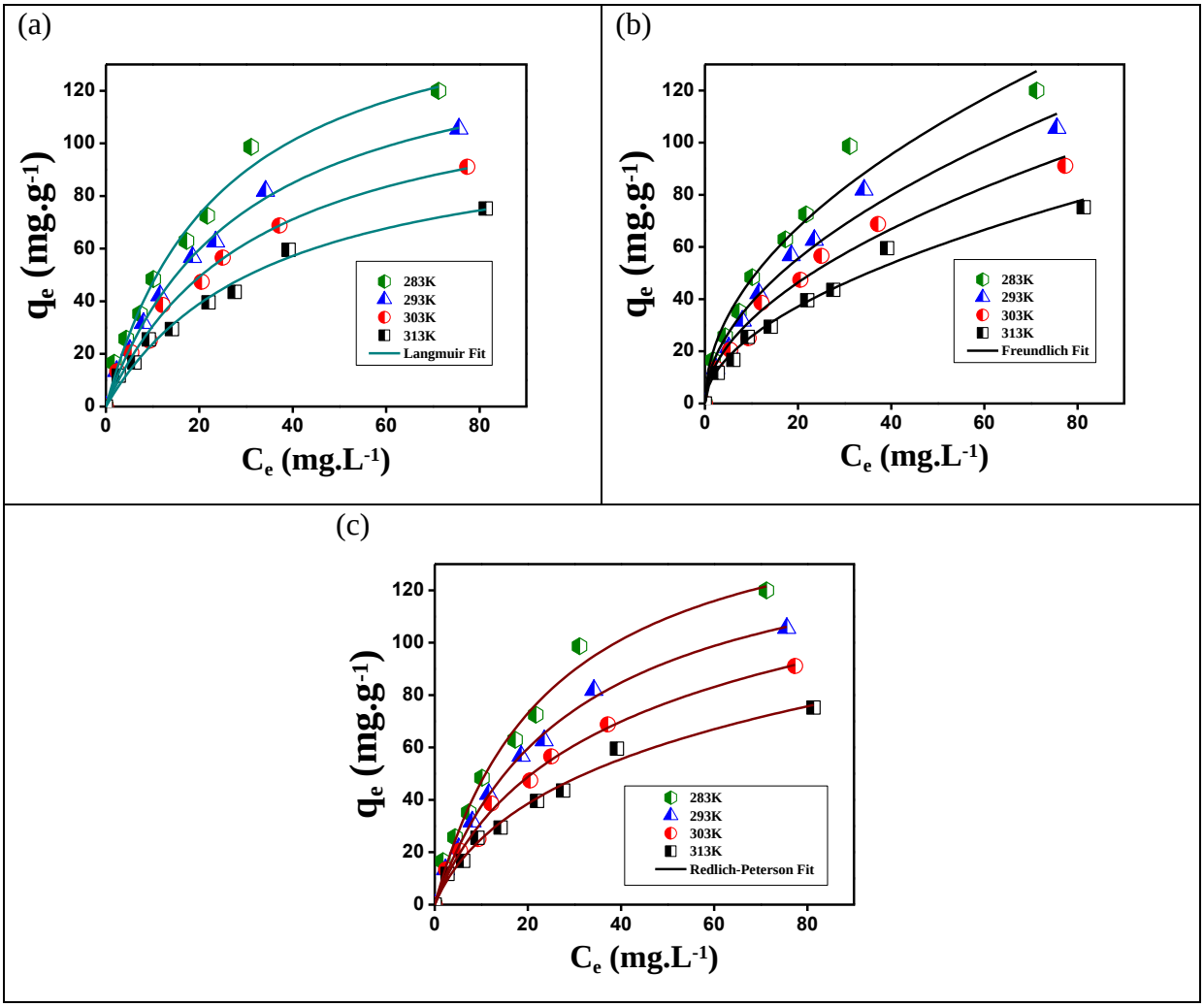

Fig. 4. Plots of equilibrium data for As(III) adsorption over HCCO surface at pH 6.0 and four different temperatures with three isotherm model (a) Langmuir, (b) Freundlich, (c) Redlich-Peterson model isotherms.

Table 6. Isotherm equation parameters estimated on As(III) adsorption for scavenging from water by HCCO at pH 6.0 and four different temperatures.

Isotherm	**Parameters**	**283K**	**293K**	**303K**	**313K**
Freundlich	**K_F(mg$^{1-1/n}$ L^n g^{-1})**	15.063	11.640	9.551	7.598
	n	1.998	1.917	1.895	1.886
	R^2	0.967	0.977	0.981	0.983

Langmuir	**q_m(mg g^{-1})**	164.011	146.791	127.905	106.970
	K_L(L mg^{-1})×10^2	0.040	0.034	0.031	0.028
	R^2	0.987	0.997	0.990	0.986
Redlich-	**A**	0.040	0.037	0.080	0.149
Peterson	**B**	6.586	5.123	4.877	4.576
	g	1	0.983	0.842	0.740
	R^2	0.985	0.996	0.989	0.987

4.1.3. Adsorption isotherm study for Cr(VI) adsorption by CHCCO

The parametric data obtained from the isotherm fits, as illustrated in Figures 5(a), 5(b), and 5(c), are compiled in Table 7 and provide valuable insights into the adsorption behavior and efficiency of the CHCCO composite material for the removal of Cr(VI). Analyzing the results reveals that the equilibrium constant (K_L) increases with temperature, indicating that the adsorption process is endothermic. This trend suggests that higher temperatures enhance the interaction between Cr(VI) ions and the CHCCO composite material, promoting more effective adsorption. Additionally, the Freundlich constant 1/n was observed to remain less than 1 at all four tested temperatures. This finding underscores the favorable nature of the adsorption process under the experimental conditions, affirming that the composite material demonstrates a high affinity for Cr(VI). Furthermore, the values of the Freundlich constant K_F showed a positive correlation with temperature, further emphasizing the increased sorption capacity of CHCCO at elevated temperatures. This temperature-dependent improvement in adsorption capacity suggests that the composite material becomes more efficient as the system is heated. The correlation coefficients (R^2) from the isotherm modeling indicate that the Freundlich model provides a superior fit to the experimental data when compared to the Langmuir model. This observation implies that the adsorption of Cr(VI) onto the CHCCO composite occurs predominantly through multilayer adsorption mechanisms rather than a uniform monolayer process. Moreover, analysis of the data fitted to the Redlich–Peterson model reveals that the g parameter deviates significantly from unity. This deviation supports the conclusion that the adsorption process takes place on heterogeneous surface sites of the CHCCO composite, further distinguishing its behavior from purely homogeneous systems.

Overall, the CHCCO composite material exhibits a high adsorption capacity for Cr(VI), particularly at higher temperatures, which enhances its performance as an adsorbent. These findings establish the composite as a highly effective material for Cr(VI) removal, making it a promising candidate for practical applications in wastewater treatment and environmental remediation.

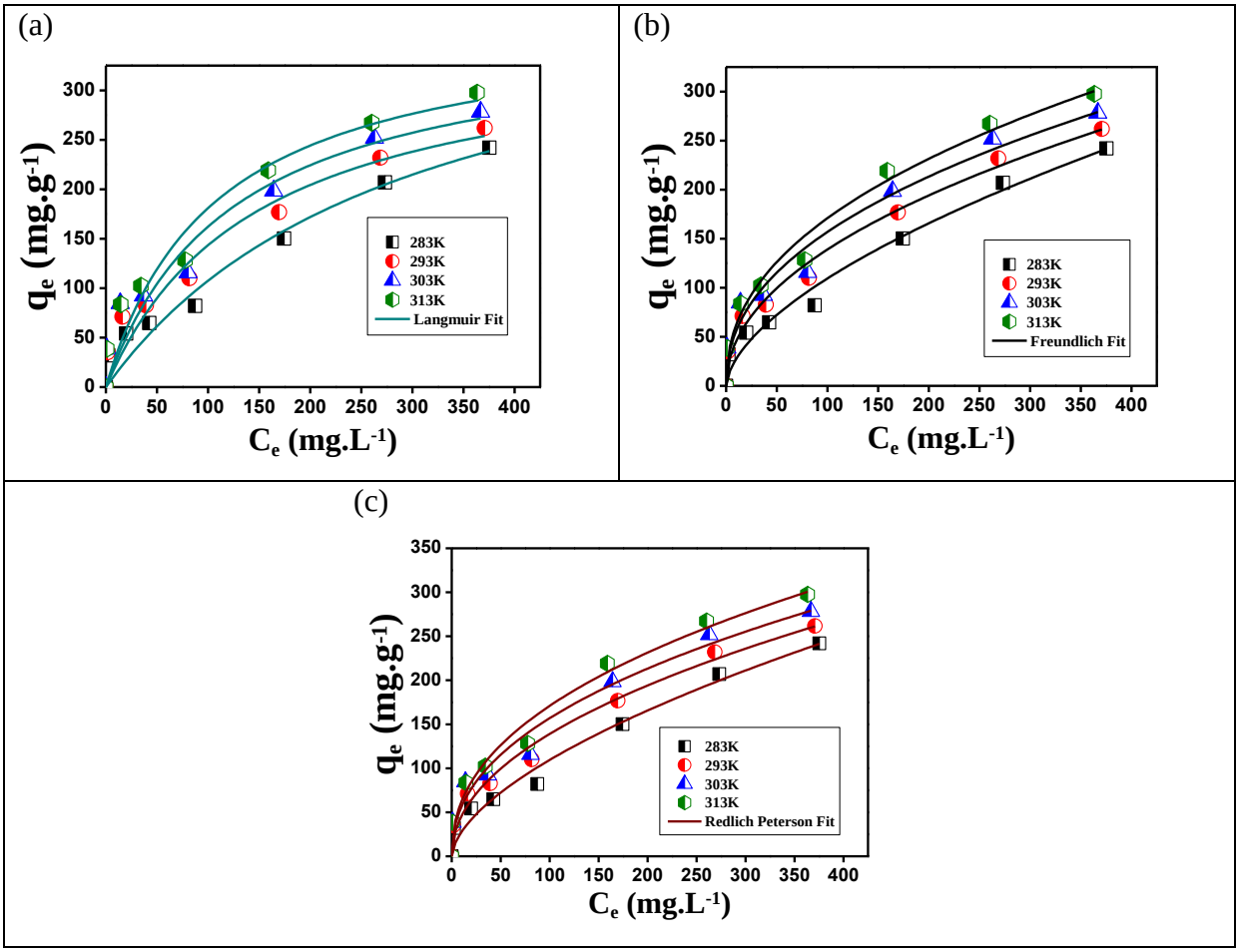

Fig. 5. The equilibrium plots for Cr(VI) adsorption over the surface of CHCCO at four different temperatures and at pH 3.0 with (a) Langmuir, (b) Freundlich, (c) Redlich-Peterson isotherm model fitting.

Table-7. Model isotherm parameters for the Cr(VI) adsorption onto CHCCO surfaces at studied four different temperatures.

Isotherm	Parameters	283K	293K	303K	313K
Freundlich	K_F(mg$^{1-1/n}$ L^n g^{-1})	6.970	15.129	20.389	22.793
	n	1.672	2.076	2.257	2.286
	R^2	0.978	0.985	0.973	0.983

Langmuir	**q_m(mg g^{-1})**	428.2	354.7	363.4	375.2
	K_L(L mg^{-1})×10^2	0.335	0.679	0.806	0.931
	R^2	0.955	0.946	0.924	0.945
Redlich-Peterson	**A×10^9**	10.205	8.594	5.781	1.481
	B×10^8	4.477	4.215	3.824	2.125
	g	0.562	0.557	0.518	0.402
	R^2	0.979	0.967	0.982	0.973

5. Summary

- A cost-efficient and highly effective nanocomposite, hydrous Ce(IV)-incorporated Cu(II) oxide (HCCO), was synthesized using a straightforward chemical process to remove Cr(VI) from polluted water. The material was thoroughly analyzed using advanced characterization techniques. It exhibited a maximum adsorption capacity of 262.89 mg·g^{-1} for an initial Cr(VI) concentration of 300 mg·L^{-1} at 313 K. The findings confirm that HCCO is an excellent adsorbent for Cr(VI) removal from wastewater.

- The hydrous Ce(IV)-incorporated Cu(II) oxide (HCCO) nanocomposite demonstrated excellent performance in eliminating As(III) from water. The adsorption process was heavily dependent on the solution's pH and adhered to a pseudo-second-order kinetic model. The equilibrium data fit well with the Langmuir isotherm model, and has a maximum adsorption capacity of 119.99 mg.g^{-1} for an initial As(III) concentration of 100 mg.L^{-1} at 283 K. These findings highlight HCCO as a highly effective and promising adsorbent for removing As(III) ions from wastewater.

- A novel composite, chitosan cross-linked hydrous Ce(IV)-incorporated Cu(II) oxide (CHCCO), was successfully synthesized through a two-step in-situ process and applied for Cr(VI) adsorption from aqueous solutions. The CHCCO composite exhibited an impressive adsorption capacity of 267.31 mg.g^{-1} at an initial Cr(VI) concentration of 300 mg.L^{-1}, pH 3, and a temperature of 313 K. These results suggest

that CHCCO holds significant potential for effectively decontaminating Cr(VI) from polluted water sources.

6. Acknowledgement

To begin, I'd want to convey my heartfelt gratitude and respects to my supervisor, Dr. Palani Sasikumar, for his steadfast assistance, essential guidance, and continuous encouragement during my research. I'd want to express my gratitude to Dr. Uday Chand Ghosh (Ex-Associate Professor, Department of Chemistry, Presidency University) for his advice, love, and unwavering support and cooperation in helping me finish my project. I would like to show my thankfulness to the University Grants Commission (UGC), Government of India, for providing me with a fellowship and financial aid. I am grateful to the Department of Chemistry at Presidency University in Kolkata, India, including the Authority, for providing the laboratory space for this research.

7. References

[1] S. Fadhil, Sustainable chromium removal by nanofiltration membranes: application of pore flow model, Int. J. Environ. Sci. Technol. 20 (2023) 8391–8398. https://doi.org/10.1007/s13762-022-04547-4.

[2] H. Ma, W. Zhou, X. Xu, X. Zhu, L. Wang, X. Shi, M. Jiang, C. Li, T. Li, Characterizing the removal of Pb^{2+} and Zn^{2+} from an acidic smelting wastewater using electrocatalytic internal Fe^{0}/C micro-electrolysis, Separation and Purification Technology 317 (2023) 123874. https://doi.org/10.1016/j.seppur.2023.123874.

[3] H.A. El-Gawad, G.K. Hassan, K.M. Aboelghait, W.H. Mahmoud, R.M. Mohamed, A.A. Afify, Removal of chromium from tannery industry wastewater using iron-based electrocoagulation process: experimental; kinetics; isotherm and economical studies, Sci Rep 13 (2023) 19597. https://doi.org/10.1038/s41598-023-46848-9.

[4] S. Li, X. Yang, Z. Wang, S. Duan, S. Zheng, X. Zheng, Effects of counterion type on selective arsenic removal process combining standard anion exchange resin with

electrocoagulation for polluted groundwater, Journal of Cleaner Production 385 (2023) 135762. https://doi.org/10.1016/j.jclepro.2022.135762.

[5] M. Xanthopoulou, I.A. Katsoyiannis, Enhanced Adsorption of Chromate and Arsenate Ions from Contaminated Water with Emphasis on Polyethylenimine Modified Materials: A Review, Separations 10 (2023) 441. https://doi.org/10.3390/separations10080441.

[6] A. Ghosh, T. Basu, B. Manna, S. Bhattacharya, U. Chand Ghosh, K. Biswas, Synthesis of a nanocomposite adsorbent with high adsorptive potential and its application for abatement of chromium(VI) from aqueous stream, Journal of Environmental Chemical Engineering 3 (2015) 565–573. https://doi.org/10.1016/j.jece.2015.01.012.

[7] A. Ghosh, M. Pal, K. Biswas, U.C. Ghosh, B. Manna, Manganese oxide incorporated ferric oxide nanocomposites (MIFN): A novel adsorbent for effective removal of Cr(VI) from contaminated water, Journal of Water Process Engineering 7 (2015) 176–186. https://doi.org/10.1016/j.jwpe.2015.06.008.

[8] L.A. Rodrigues, L.J. Maschio, R.E. da Silva, M.L.C.P. da Silva, Adsorption of Cr(VI) from aqueous solution by hydrous zirconium oxide, Journal of Hazardous Materials 173 (2010) 630–636. https://doi.org/10.1016/j.jhazmat.2009.08.131.

[9] S. Goswami, S.C. Bhat, U.C. Ghosh, Crystalline Hydrous Ferric Oxide: An Adsorbent for Chromium(VI)-Contaminated Industrial Wastewater Treatment, Water Environment Research 78 (2006) 986–993. https://doi.org/10.2175/106143005X73604.

[10] Y. Wang, D. Liu, J. Lu, J. Huang, Enhanced adsorption of hexavalent chromium from aqueous solutions on facilely synthesized mesoporous iron–zirconium bimetal oxide, Colloids and Surfaces A: Physicochemical and Engineering Aspects 481 (2015) 133–142. https://doi.org/10.1016/j.colsurfa.2015.01.060.

[11] A.S. Mahmoud, N.Y. Mohamed, M.K. Mostafa, M.S. Mahmoud, Effective Chromium Adsorption From Aqueous Solutions and Tannery Wastewater Using Bimetallic Fe/Cu Nanoparticles: Response Surface Methodology and Artificial Neural Network, Air, Soil and Water Research 14 (2021) 11786221211028162. https://doi.org/10.1177/11786221211028162.

[12] V.K. Gupta, R. Chandra, I. Tyagi, M. Verma, Removal of hexavalent chromium ions using CuO nanoparticles for water purification applications, Journal of Colloid and Interface Science 478 (2016) 54–62. https://doi.org/10.1016/j.jcis.2016.05.064.

[13] J. Matusik, J. Hyla, P. Maziarz, K. Rybka, T. Leiviskä, Performance of Halloysite-Mg/Al LDH Materials for Aqueous As(V) and Cr(VI) Removal, Materials 12 (2019) 3569. https://doi.org/10.3390/ma12213569.

[14] S. Recillas, J. Colón, E. Casals, E. González, V. Puntes, A. Sánchez, X. Font, Chromium VI adsorption on cerium oxide nanoparticles and morphology changes during the process, Journal of Hazardous Materials 184 (2010) 425–431. https://doi.org/10.1016/j.jhazmat.2010.08.052.

[15] W. Weilong, F. Xiaobo, Efficient Removal of Cr(VI) with Fe/Mn Mixed Metal Oxide Nanocomposites Synthesized by a Grinding Method, Journal of Nanomaterials 2013 (2013) 1–8. https://doi.org/10.1155/2013/514917.

[16] L. Zhang, W. Xia, B. Teng, X. Liu, W. Zhang, Zirconium cross-linked chitosan composite: Preparation, characterization and application in adsorption of Cr(VI), Chemical Engineering Journal 229 (2013) 1–8. https://doi.org/10.1016/j.cej.2013.05.102.

[17] W. Zhang, S. Zhang, J. Wang, M. Wang, Q. He, J. Song, H. Wang, J. Zhou, Hybrid functionalized chitosan-Al_2O_3@SiO_2 composite for enhanced Cr(VI) adsorption, Chemosphere 203 (2018) 188–198. https://doi.org/10.1016/j.chemosphere.2018.03.188.

[18] L. Zhang, W. Xia, X. Liu, W. Zhang, Synthesis of titanium cross-linked chitosan composite for efficient adsorption and detoxification of hexavalent chromium from water, J. Mater. Chem. A 3 (2015) 331–340. https://doi.org/10.1039/C4TA05194G.

[19] R. El Kaim Billah, A. Shekhawat, S. Mansouri, H. Majdoubi, M. Agunaou, A. Soufiane, R. Jugade, Adsorptive removal of Cr(VI) by Chitosan-SiO_2-TiO_2 nanocomposite, Environmental Nanotechnology, Monitoring & Management 18 (2022) 100695. https://doi.org/10.1016/j.enmm.2022.100695.

[20] Y. Xiao, H. Liang, Z. Wang, $MnFe_2O_4$/chitosan nanocomposites as a recyclable adsorbent for the removal of hexavalent chromium, Materials Research Bulletin 48 (2013) 3910–3915. https://doi.org/10.1016/j.materresbull.2013.05.099.

[21] W. Xu, J. Wang, L. Wang, G. Sheng, J. Liu, H. Yu, X.-J. Huang, Enhanced arsenic removal from water by hierarchically porous CeO_2–ZrO_2 nanospheres: Role of surface- and structure-dependent properties, Journal of Hazardous Materials 260 (2013) 498–507. https://doi.org/10.1016/j.jhazmat.2013.06.010.

[22] T. Luo, J. Cui, S. Hu, Y. Huang, C. Jing, Arsenic Removal and Recovery from Copper Smelting Wastewater Using TiO_2, Environ. Sci. Technol. 44 (2010) 9094–9098. https://doi.org/10.1021/es1024355.

[23] C.A. Martinson, K.J. Reddy, Adsorption of arsenic(III) and arsenic(V) by cupric oxide nanoparticles, Journal of Colloid and Interface Science 336 (2009) 406–411. https://doi.org/10.1016/j.jcis.2009.04.075.

[24] R. Li, Q. Li, S. Gao, J.K. Shang, Exceptional arsenic adsorption performance of hydrous cerium oxide nanoparticles: Part A. Adsorption capacity and mechanism, Chemical Engineering Journal 185–186 (2012) 127–135. https://doi.org/10.1016/j.cej.2012.01.061.

[25] Z. Li, S. Deng, G. Yu, J. Huang, V.C. Lim, As(V) and As(III) removal from water by a Ce–Ti oxide adsorbent: Behavior and mechanism, Chemical Engineering Journal 161 (2010) 106–113. https://doi.org/10.1016/j.cej.2010.04.039.

[26] Z. Ren, G. Zhang, J. Paul Chen, Adsorptive removal of arsenic from water by an iron–zirconium binary oxide adsorbent, Journal of Colloid and Interface Science 358 (2011) 230–237. https://doi.org/10.1016/j.jcis.2011.01.013.

[27] Y. Babaee, C.N. Mulligan, M.S. Rahaman, Removal of arsenic (III) and arsenic (V) from aqueous solutions through adsorption by Fe/Cu nanoparticles, J of Chemical Tech & Biotech 93 (2018) 63–71. https://doi.org/10.1002/jctb.5320.

[28] S. Liu, S. Kang, G. Wang, H. Zhao, W. Cai, Micro/nanostructured porous Fe–Ni binary oxide and its enhanced arsenic adsorption performances, Journal of Colloid and Interface Science 458 (2015) 94–102. https://doi.org/10.1016/j.jcis.2015.07.038.

[29] W. Zhang, C. Liu, T. Zheng, J. Ma, G. Zhang, G. Ren, L. Wang, Y. Liu, Efficient oxidation and sorption of arsenite using a novel titanium(IV)-manganese(IV) binary oxide sorbent, Journal of Hazardous Materials 353 (2018) 410–420. https://doi.org/10.1016/j.jhazmat.2018.04.034.

[30] Y. Li, D. Zhang, W. Li, Y. Lan, Y. Li, Efficient removal of As(III) from aqueous solution by S-doped copper-lanthanum bimetallic oxides: Simultaneous oxidation and adsorption, Chemical Engineering Journal 384 (2020) 123274. https://doi.org/10.1016/j.cej.2019.123274.

[31] G. Zhang, A. Khorshed, J. Paul Chen, Simultaneous removal of arsenate and arsenite by a nanostructured zirconium–manganese binary hydrous oxide: Behavior and mechanism, Journal of Colloid and Interface Science 397 (2013) 137–143. https://doi.org/10.1016/j.jcis.2012.11.056.

[32] B.R. Manna, S. Dey, S. Debnath, U.C. Ghosh, Removal of Arsenic from Groundwater using Crystalline Hydrous Ferric Oxide (CHFO), Water Quality Research Journal 38 (2003) 193–210. https://doi.org/10.2166/wqrj.2003.013.

[33] K. Gupta, U.C. Ghosh, Arsenic removal using hydrous nanostructure iron(III)–titanium(IV) binary mixed oxide from aqueous solution, Journal of Hazardous Materials 161 (2009) 884–892. https://doi.org/10.1016/j.jhazmat.2008.04.034.

[34] W. Zhang, C. Liu, L. Wang, T. Zheng, G. Ren, J. Li, J. Ma, G. Zhang, H. Song, Z. Zhang, Z. Li, A novel nanostructured Fe-Ti-Mn composite oxide for highly efficient arsenic removal: Preparation and performance evaluation, Colloids and Surfaces A: Physicochemical and Engineering Aspects 561 (2019) 364–372. https://doi.org/10.1016/j.colsurfa.2018.10.077.

[35] A. Gupta, V.S. Chauhan, N. Sankararamakrishnan, Preparation and evaluation of iron–chitosan composites for removal of As(III) and As(V) from arsenic contaminated real life groundwater, Water Research 43 (2009) 3862–3870. https://doi.org/10.1016/j.watres.2009.05.040.

[36] J.M. Aguirre, A. Gutiérrez, O. Giraldo, Simple route for the synthesis of copper hydroxy salts, J. Braz. Chem. Soc. 22 (2011) 546–551. https://doi.org/10.1590/S0103-50532011000300019.

[37] A.B. Albadarin, Z. Yang, C. Mangwandi, Y. Glocheux, G. Walker, M.N.M. Ahmad, Experimental design and batch experiments for optimization of Cr(VI) removal from aqueous solutions by hydrous cerium oxide nanoparticles, Chemical Engineering Research and Design 92 (2014) 1354–1362. https://doi.org/10.1016/j.cherd.2013.10.015.

[38] J. Lin, L. Fan, R. Miao, X. Le, S. Chen, X. Zhou, Enhancing catalytic performance of laccase via immobilization on chitosan/CeO_2 microspheres, International Journal of Biological Macromolecules 78 (2015) 1–8. https://doi.org/10.1016/j.ijbiomac.2015.03.033.

Lists of Publications

1) **Ayan Ghosh**, Sumana Mondal, Sarat Kanrar, Ankur Srivastava, Mrituanjay D. Pandey, Uday Chand Ghosh, Palani Sasikumar. Efficient removal of chromate from wastewater using a one-pot synthesis of chitosan cross-linked ceria incorporated hydrous copper oxide bio-polymeric composite, International Journal of Biological Macromolecules 276 (2024) 134016. **https://doi.org/10.1016/j.ijbiomac.2024.134016.**

2) **Ayan Ghosh**, Sarat Kanrar, Ankur Srivastava, Mrituanjay D. Pandey, Uday Chand Ghosh, Palani Sasikumar. Hexavalent chromium scavenging performances of one-pot synthesized hydrous cerium-copper-mixed oxide from contaminated water with plausible mechanism, Separation Science and Technology 59 (2024) 1405–1424. **https://doi.org/10.1080/01496395.2024.2372418**
3) Sweta Maji, **Ayan Ghosh**, Kaushik Gupta, Abir Ghosh, Uttam Ghorai, Angshuman Santra, Palani Sasikumar, Uday Chand Ghosh. Efficiency evaluation of arsenic (III) adsorption of novel graphene oxide@ iron-aluminium oxide composite for the contaminated water purification, Separation and Purification Technology 197 (2018) 388-400. **https://doi.org/10.1016/j.seppur.2018.01.021**
4) Sarat Kanrar, **Ayan Ghosh**, Abir Ghosh, Srikanta Chowdhury, Mriganka Sadhukhan, Uday Chand Ghosh, Palani Sasikumar. Tailored hybrid Ce-Zr-La hydrous oxide material: Preparation, characterization and application towards removal of fluoride and copper (II) from their contaminated water. Inorganic Chemistry Communications. 158 (2023) 111381. **https://doi.org/10.1016/j.inoche.2023.111381**
5) Sarat Kanrar, Abir Ghosh, **Ayan Ghosh**, Mriganka Sadhukhan, Tanmay Bhowmik, Uday Chand Ghosh, Palani Sasikumar. Facile synthesis and characterization of chromium (III)/zirconium (IV) impregnated chitosan/β-cyclodextrin bio-composite and application towards efficient removal of copper (II) from aqueous systems. Inorganic Chemistry Communications. 145 (2022) 109988. **https://doi.org/10.1016/j.inoche.2022.109988**
6) Sarat Kanrar, Abir Ghosh, **Ayan Ghosh**, Arpan Mondal, Mriganka sadhukhan, Uday Chand Ghosh, Sasikumar Palani, One-pot synthesis of Cr(III)-incorporated Zr(IV) oxide for fluoride remediation: a lab to field performance evaluation study, Environmental Science and Pollution Research 27 (2020) 15029–15044. **https://doi.org/10.1007/s11356-020-07980-5**

National & International Seminar, Conference & Workshop Presentation

1. Research paper presented for the poster presentation on **8-9th January, 2020** in **Two-day International seminar on " Innovation, Expansion, Impacts and Challenges**

in Chemical and Biological Sciences," organized by Department of Chemistry, Surendranath College.

2. Research paper presented for the oral presentation on **December 23-24, 2019** in **4th Regional Science and Technology Congress (Southern Regeion)**, organized by Department of science & technology and bio-technology, Govt.of West Bengal &MaulanaAbulKalam Azad University of Technology, West Bengal at Haringhata, Nadia.

3. Research paper presented for the poster presentation on **March 28, 2023** in **One Day National Symposium on Frontiers in Chemistry: from Fundamentals to Application** organized by the Department of Chemistry, Presidency University, Kolkata.

4. Research paper presented for the Poster presentation on **18-19th November, 2022** at **National Seminar on Environmental Sustainability: Issues and Challenges** organized by Sripat Singh College, Jiaganj, Murshidabad and sponsored by Department of Science & Technology and Biotechnology (DSTBT), Govt. of West Bengal.

5. Research paper presented for the Poster presentation on **20-21st December, 2019** in **SERB-DST, BRNS, CSIR, and MoES** sponsored **11th National Conference on Solid State Chemistry and Allied Areas (NCSCA-2019)** held at Nagpur, India.

Chhanda Mukhopadhyay 04/03/25

Ayan Ghosh

Signature of the candidate

(AYAN GHOSH)

Forwarded

(Dr. PALANI SASIKUMAR)

Supervisor

Assistant Professor of Chemistry

Presidency University, Kolkata

Dr. Sasikumar Palani
Assistant Professor
Department of Chemistry
Presidency University, Kolkata-700 073